A microfluidic device for on-chip agarose microbead generation with ultralow reagent consumption

Linda Desbois, Adrien Padirac, Shohei Kaneda, Anthony J. Genot, Yannick Rondelez, Didier Hober, Dominique Collard, and Teruo Fujii

Citation: Biomicrofluidics **6**, 044101 (2012); doi: 10.1063/1.4758460
View online: http://dx.doi.org/10.1063/1.4758460
View Table of Contents: http://scitation.aip.org/content/aip/journal/bmf/6/4?ver=pdfcov
Published by the AIP Publishing

A microfluidic device for on-chip agarose microbead generation with ultralow reagent consumption

Linda Desbois,[1] Adrien Padirac,[1] Shohei Kaneda,[1] Anthony J. Genot,[1] Yannick Rondelez,[1] Didier Hober,[2] Dominique Collard,[1] and Teruo Fujii[1,a)]
[1]*LIMMS/CNRS-IIS, Institute of Industrial Science, The University of Tokyo, 4-6-1 Komaba, Meguro-ku, Tokyo 153-8505, Japan*
[2]*Université Lille 2, Faculté de Médecine et CHRU Lille, Laboratoire de Virologie/EA 3610, Loos-lez-lille 59120, France*

(Received 23 July 2012; accepted 27 September 2012; published online 9 October 2012)

Water-in-oil microdroplets offer microreactors for compartmentalized biochemical reactions with high throughput. Recently, the combination with a sol-gel switch ability, using agarose-in-oil microdroplets, has increased the range of possible applications, allowing for example the capture of amplicons in the gel phase for the preservation of monoclonality during a PCR reaction. Here, we report a new method for generating such agarose-in-oil microdroplets on a microfluidic device, with minimized inlet dead volume, on-chip cooling, and *in situ* monitoring of biochemical reactions within the gelified microbeads. We used a flow-focusing microchannel network and successfully generated agarose microdroplets at room temperature using the "push-pull" method. This method consists in pushing the oil continuous phase only, while suction is applied to the device outlet. The agarose phase present at the inlet is thus aspirated in the device, and segmented in microdroplets. The cooling system consists of two copper wires embedded in the microfluidic device. The transition from agarose microdroplets to microbeads provides additional stability and facilitated manipulation. We demonstrate the potential of this method by performing on-chip a temperature-triggered DNA isothermal amplification in agarose microbeads. Our device thus provides a new way to generate microbeads with high throughput and no dead volume for biochemical applications. © *2012 American Institute of Physics*. [http://dx.doi.org/10.1063/1.4758460]

I. INTRODUCTION

Microfluidic technologies are based on the use of liquid flows in small volumes, with the benefit of reducing reagent volume, mitigating sample contamination, and providing a high throughput system for the integration of multiple functions in *micrototal analysis systems* (μTAS). Water-in-oil microdroplets allow the generation of microreactors (pl to fl volume), which permits the compartmentalization of reactions for multiple chemical and biochemical applications such as protein crystallization,[1] organic molecule[2] or nanoparticle synthesis,[3] genome sequencing,[4] and single cell and single molecule analysis.[5–7] With respect to molecular biology operations, previous work showed the efficiency of reagents compartmentalization for polymerase chain reaction (PCR),[8,9] single cell analysis,[10–12] or transcriptome analysis.[13] Generation of monodisperse microdroplets[12] is one way to carry out high throughput analysis[14] and execute independent reactions in parallel.[9]

Recently developed agarose microdroplets have been used to compartmentalize PCR[15,16] and reverse transcription polymerase chain reaction (RT-PCR) from cellular mRNA.[13] These reports take advantage of the thermo-responsive sol-gel switching property of agarose to trap amplicons in the agarose gel matrix, allowing the preservation of monoclonality of products within stable agarose microbeads. Actually, long-term stability of microdroplets is an important

a)Author to whom correspondence should be addressed. Electronic mail: tfujii@iis.u-tokyo.ac.jp.

requirement for their storage and downstream applications, such as fluorescence activated cell sorting (FACS) analysis and RNA sequencing for single cell transcriptome analysis.

However, usual protocols described in the literature highlight two critical points associated with the generation and use of agarose microbeads. The first one is to avoid unexpected gelation upstream of the droplet formation process. This is typically addressed with a heating system adapted to the reagent syringe.[17,18] The second one is the delicate operation of microdroplets; imperfectly stabilized droplets can recoalesce[19] during storage, incubation, and collection, before they are cooled into microbeads[17] and sent to downstream applications.[13,16]

Here, we have developed an integrated device for completely on-chip operations using agarose microbeads. The specific features of our device are (i) the "push-pull" microdroplet generation system that drastically downscales reagent consumption and (ii) the integration of the heating/cooling system necessary to turn agarose microdroplets into microbeads immediately after their formation. We demonstrate the suitability of our device by performing and monitoring on-chip a DNA isothermal amplification reaction within the device.

The basic structure is a flow-focusing microchannel network for microdroplet generation. We propose a new way to handle the fluids to generate microdroplets: the "push-pull" operation. The oil mix, on the one hand, is pushed into the device. Suction (i.e., a negative flow rate) is applied at the outlet with a higher rate than the oil inlet flow rate: this induces aspiration of the agarose sample and its segmentation into monodisperse microdroplets. Because there is no tubing associated with the sample inlet, the dead volume is drastically reduced and the consumption of sample can be decreased to only a few microliters.

A pair of copper wires are embedded in the microfluidic chip and connected to a heat sink. After enough agarose-in-oil microdroplets have been formed, this cooling system is used to gelify them into agarose microbeads.

In order to validate our setup for biochemical applications, we prepared a DNA amplification mixture containing 1.5% agarose and successfully observed temperature triggered DNA isothermal amplification within such microbeads.

This sequence of operations is performed entirely in a single chip and described in more details below.

II. MATERIALS AND METHODS

A. Design and fabrication of the microfluidic device

The microchannel network is designed with AUTOCAD software and then reproduced to a chromium mask.

The device mold is made using a standard soft photolithography technique.[20,21] Briefly, 70 μm SU-8 2050 negative photoresist (Microchem, Japan) is spin-coated on a silicon wafer. The mask is fixed on the top of the photoresist coat, which is then photocured by UV exposure. After development, the mold is coated with a Teflon plasma. Then, some polydimethylsiloxane (PDMS) is poured on the mold and baked at 75 °C during 1.5 h. The polymerized PDMS sheet is peeled off and cut in rectangular chips. O_2 plasma treatment is performed with a RIE machine to allow PDMS/glass bonding. The PDMS chip with the microchannel network is bonded to a 24 mm × 36 mm × 150 μm glass slide. Silicone connecting tubes are introduced in the inlet and outlet of the PDMS chip, and sealed with PDMS.

B. Agarose microdroplet generation at room temperature (25 °C)

After 10 min degassing in a vacuum chamber, the device is filled with water. A 1 ml syringe (Terumo, Japan) containing the oil mix is connected to the oil inlet, and the continuous phase is pushed into the device. Another 1 ml syringe containing water is connected to the outlet, and suction is applied to induce the aspiration of the emulsion.

The oil mix (Mineral oil, Sigma, Japan) prepared with surfactants to prevent microdroplet coalescence is made with 2% silicone based polymeric surfactant ABIL-EM 90 (Goldschmidt, Essen, Germany) and 0.05% Triton 100 X (Sigma, Japan).

The DNA amplification reagents are suspended in a 1.5% agarose solution (ultra-low gelling agarose type XI-A, Sigma, Japan). A small volume of this mix is dispensed in the inlet well with a micropipette (Gilson, France).

The flow-focusing microfluidic device consists of a cross junction with two 25 μm thick oil channels perpendicular to the agarose channel (Figure 1). In the orthogonal nozzle, the oil phase, focusing on the aspirated agarose stream, segments the disperse phase in regular 55 μm microdroplets.

The generation of these microdroplets is observed with an inverted microscope (Olympus IX 71, Japan) and their diameters are analyzed off-line with the software IMAGEJ, in order to assess the dispersity of the emulsion (the measurement error is $\pm$ 0.5 μm).

C. On-chip agarose microdroplet cooling into agarose microbeads

PDMS is perforated with a needle 550 μm in diameter, about 500 μm away from the incubation chamber walls, on the device (Figure 3). Two copper wires 550 μm in diameter are introduced in place of the needle in the PDMS. 3 cm, 4 cm, 5 cm, 6 cm, 8 cm, and 10 cm long copper wires have been tested. Once the observation chamber is filled with agarose microdroplets, the syringe pumps are stopped, and the wires are cooled at 0 °C in ice. After agarose gelation has occurred, the microbeads are heated back to 43 °C with a thermoplate (Tokai, Japan) for DNA isothermal amplification. Because this temperature is below the melting temperature of 1.5% agarose (60 °C), the beads remain in the gel state during this process.

D. Temperature measurement in the device

Temperature is measured with a K-type thermocouple (NI USB-TC01 model, National instruments, Japan) inserted in the middle of the incubation chamber (Figure 3). Temperature is measured every minute during 10 min in the device containing either no cooling wires or a pair of copper wires with a length ranging from 4 to 10 cm. Temperature curves are plotted with Kaleida graph (SYNERGY software).

The variations of the temperature in the incubation chamber have been simulated with COMSOL MULTIPHYSICS software and are shown in supplemental material.[28]

E. DNA amplification reaction

Reactions are done in a buffer containing 10 mM KCl, 10 mM $(NH_4)_2SO_4$, 50 mM NaCl, 2 mM $MgSO_4$, 45 mM Tris–HCl, 5 mM $MgCl_2$, 6 mM DTT, 100 μg/ml bovine serum albumin

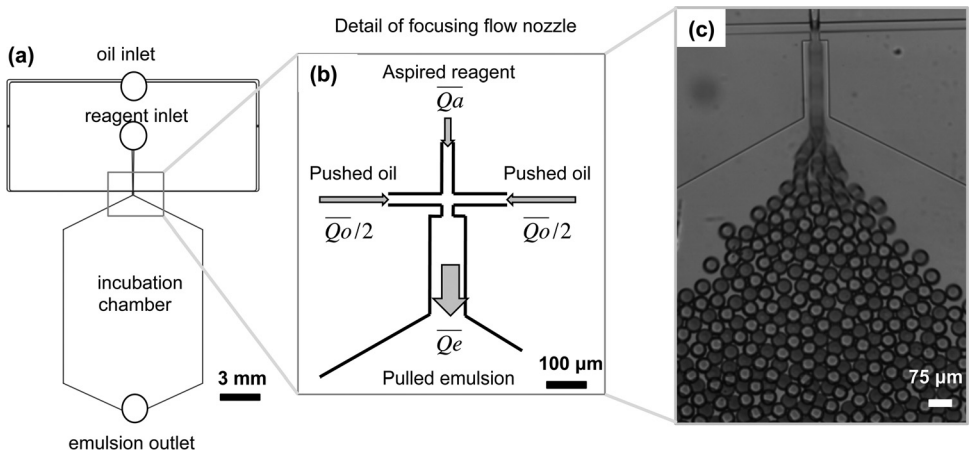

FIG. 1. Microfluidic device for agarose microdroplet generation at room temperature. (a) General view of the device. (b) The oil continuous phase is pushed while the emulsion is pulled. (c) This system induces segmentation of the agarose stream into monodisperse agarose microdroplets.

(New England Biolabs), and dNTPs (100 μM each). *Bst* DNA polymerase, large fragment, and NtBstNBI nicking endonuclease are purchased from New England Biolabs and used at 11.2 U/ml and 200 U/ml, respectively.

DNA oligonucleotides were purchased from Integrated DNA Technologies (IDT, Coralville, IA, USA), with high performance liquid chromatography purification. For the amplification reaction, 300 nM of a template strand (5′-AACAGACTCGAAACAGACTCGA-3′) with a 3′-terminal TAMRA NHS ester modification is put in the presence of 300 nM of an inhibitor strand (5′-GTCTGTTTCGAGTAA-3′) and 0.01 nM of an input strand (5′-TCGAGTCTGTT-3′).

Control reactions have been performed in 0.5% to 2% of agarose (Ultra-low gelling agarose type XI-A, Sigma, Japan) and are shown in supplemental material.[28]

10 μl of the reaction mixture were introduced in the device for amplification at 43 °C in agarose microbeads. Another 10 μl were run in a CFX96 real-time thermocycler (Bio-Rad), set at the same constant temperature, for control.

F. DNA amplification monitoring and DNA amplification curve

Microbeads are illuminated with a 490 nm light emitting diode (LED) light source (CoolLED, pE excitation system, UK). They are observed through a Cy3-4040C filter cube (Semrock Corp.) in order to detect the fluorescence emitted by TAMRA.

Images are recorded with an Andor XION camera, using μMANAGER software.[22]

The fluorescence of 10 drops is measured with IMAGEJ software, every 2 min, during 120 min. The measured fluorescence of the on-chip and control (bulk) reactions is normalized at 0 for the lowest and 1 for the highest fluorescence intensity. For the on-chip amplification, the mean fluorescence of 10 drops ± standard deviation is plotted.

III. RESULTS AND DISCUSSION

Previous reports described the application of the sol-to-gel switching properties of agarose to make agarose microbeads, with applications to RT-PCR from cellular mRNA[13] or cell encapsulation. These reports used a pushing system, and the gelation of the agarose was performed off-chip. To mitigate issues associated with droplet coalescence during their manipulation, we investigated the integrated generation of agarose microdroplets at room temperature, and gelation on-chip into microbeads. Our method has the additional advantage of a very low volume consumption of reagents.

A. Agarose microdroplet generation at room temperature with an ultra low volume of sample

In order to check the feasibility of droplet generation at room temperature (25 °C), we designed a network of flow-focusing microchannels.

The oil mix, containing silicone-based ABIL-EM90 surfactants to avoid unexpected droplet coalescence, is pushed with a syringe pump with a $\overline{Qo} = 4$ μl/min flow rate. At the same time, 10 μL of 1.5% agarose solution are deposited onto the reagent inlet. To induce agarose flow focusing in the nozzle and stream segmentation (i.e., the generation of an emulsion), suction is applied at the outlet with a $\overline{Qe} = 5$ μl/min flow rate. The applied pulling flow at the outlet induced the aspiration of the agarose solution, stream focusing in the nozzle (Figure 1(b)) and segmentation by the perpendicular oil stream: thus, the microemulsion is generated.

As shown in Figure 1(c), highly monodisperse microdroplets 55 μm in diameter are produced. Considering ($\overline{Qa}$), the agarose flow rate ($\overline{Qa} = \overline{Qe} - \overline{Qo}$), and the microdroplet size (55 μm in diameter), we estimated the microdroplet flow generation at 250 Hz.

By tuning the inlet and the outlet flow rates, we could easily control the droplet diameter and the type of droplet regime formation.[23] For example, we could generate microdroplets 20 μm in diameter in the jetting regime at 3900 Hz (Figure 2(a)). Microdroplets present an uniform diameter of 20 μm ± 3 μm (Figure 2(d)). We could also generate, in the dripping regime, monodisperse microemulsions with diameters of 35 or 50 μm (Figures 2(b) and 2(c)).

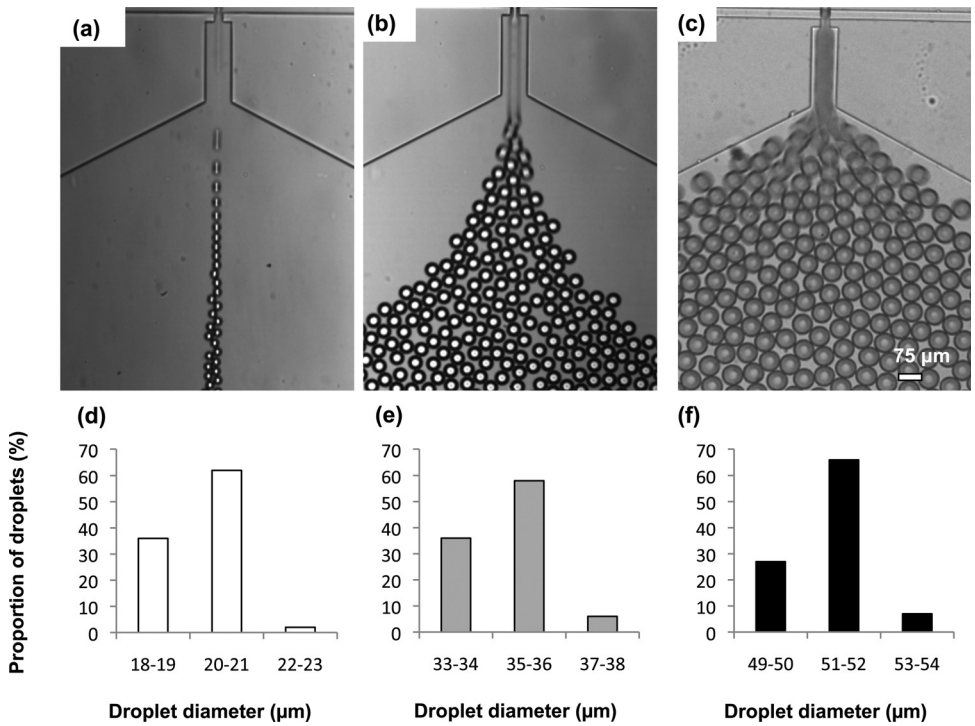

FIG. 2. Different regimes of microdroplet generation and microemulsion polydispersity. By tuning the oil and outlet flow, the diameter of droplets can be changed: (a) 20 μm, (b) 35 μm, (c) 50 μm. In the case of an agarose flow rate of 1 μL/min, the microdroplet generation frequency varies from 3900 Hz for (a) 20 μm microdroplets to (c) 200 Hz for 50 μm microdroplets. (d)-(f) Polydispersity of microdroplets.

B. On-chip agarose microbead gelation

We investigated a way to cool agarose microdroplets into agarose microbeads on-chip, for easy off-chip collection and direct use for downstream applications.

The 1.5% ultralow gelling type IX-A agarose melts at 60 °C, and its sol-to-gel switch transition occurs at $\leq$ 17 °C. The purpose is to decrease the temperature to this critical gelling temperature in the incubation chamber of the device.

Using the high thermal conductivity of copper, we designed a system to cool the chamber. For this, we introduced two copper wires on both sides of the incubation chamber.

At first, we characterized the temperature in the incubation chamber. We introduced a K-type gauge thermocouple in the incubation chamber as shown in Figure 3. In order to avoid any leakage after introduction, the thermocouple was sealed with PDMS and baked at 75 °C during 1.5 h.

Microdroplets are generated, as mentioned above, at room temperature. When the incubation chamber is filled with microdroplets, inlet and outlet flows are stopped, and we proceed to the cooling stage.

For this, the two copper wires are introduced in two 1 ml tubes containing ice (0 °C). To characterize the thermal behavior of the reactor, cooling was carried out with copper wires of different length, as shown in the Figure 3. The temperature trends are plotted in Figure 4(a): they reach the steady state in 10 min, irrespective of wire length.

The chamber can be modeled by a thermal capacity, with 2 heat sinks, one associated with room temperature (thermal resistivity: R_{RT}) and the second one with the cooling system. The electro-thermal equivalent is plotted in the insert of Figure 4(b). The heat transfer with the cold point (ice) is determined by the wire thermal conductivity, serially connected to the wire/chamber resistivity. The evolution of the thermal resistivity of the cooling system with the wire length is plotted in Figure 4(b), from steady state values shown in Figure 4(a). The linear dependence

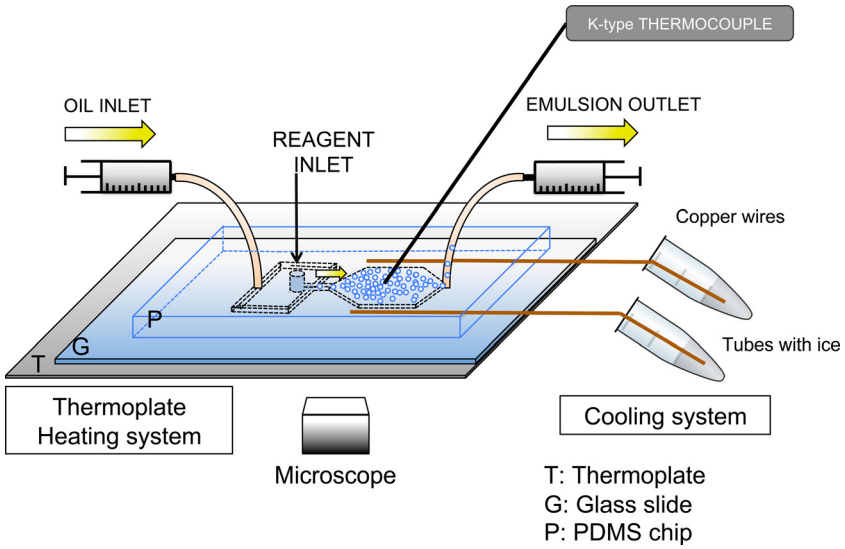

FIG. 3. Device set-up for microbead generation. The "push-pull" method allows the generation of a stable microemulsion. The temperature is measured with A K-type thermocouple, introduced and sealed in the incubation chamber. Heating is done with a thermoplate. Two copper wires introduced in 1 mL tubes filled with ice are used as a heat sink.

of the wire conductivity with its length is clearly obtained, and the slope $(\lambda.S.R_{RT})^{-1}$ allows us the calculation of the thermal resistances of the models. λ is the thermal conductivity of copper ($3.9\,W\,cm^{-1}\,K^{-1}$) and S the wire cross-section ($2.5 \times 10^{-4}\,cm^2$). To complete the model identification, the thermal capacitance of the chamber is deduced from the cooling dynamics with a short wire (4 cm), as shown in Figure 4(c).

Simulations made with COMSOL (see supplemental material)[28] show that the temperature in the chamber is homogeneous with a 1.3 °C variation from the wall chamber to the center (supplemental material, Fig. S1).[28] With this set-up, an 16 mm wide chamber can be cooled below 17 °C (supplemental material, Fig. S2).[28]

This analysis confirmed that we could reach the gelation temperature of agarose within the chamber. We experimentally validated the correct gelation of microdroplets into microbeads by considering the transparency of the microdroplets before and after cooling. As shown on the Figure 5(a), after generation, agarose microdroplets were transparent: this limpidity is correlated to the liquid state of the solution.[24]

After 15 min of cooling at 14 °C, the aspect of the microdroplets changed unambiguously and they became opaque as shown in Figure 5(b). As previously reported, during the gelation process, the turbidity of the gel increases with the apparition of a three-dimensional network of agarose fibers.[24] Considering the temperature of the sol-to-gel transition ($\leq$17 °C) and the fact that agarose gelation increases the microdroplets' opacity, we considered that agarose microdroplets were successfully cooled, and agarose microbeads were formed.

C. DNA amplification and monitoring on-chip

To confirm the reliability of our system, we used an EXPAR-like isothermal DNA amplification reaction.[25] A "template" strand enables the autocatalytic amplification of the target strand α (Figure 6(a)). As α hybridizes to the template in 3′ position, it is elongated by a DNA polymerase. The elongated strand is then cut in its middle by a nicking endonuclease, releasing two α strands.

We monitor the reaction with N-quenching, a versatile fluorescent technique to observe the hybridization of DNA strands:[26] the 3′ end of the template is labeled with a single fluorophore (TAMRA), whose fluorescence intensity increases as α hybridizes to the template as shown in Figure 6(a).

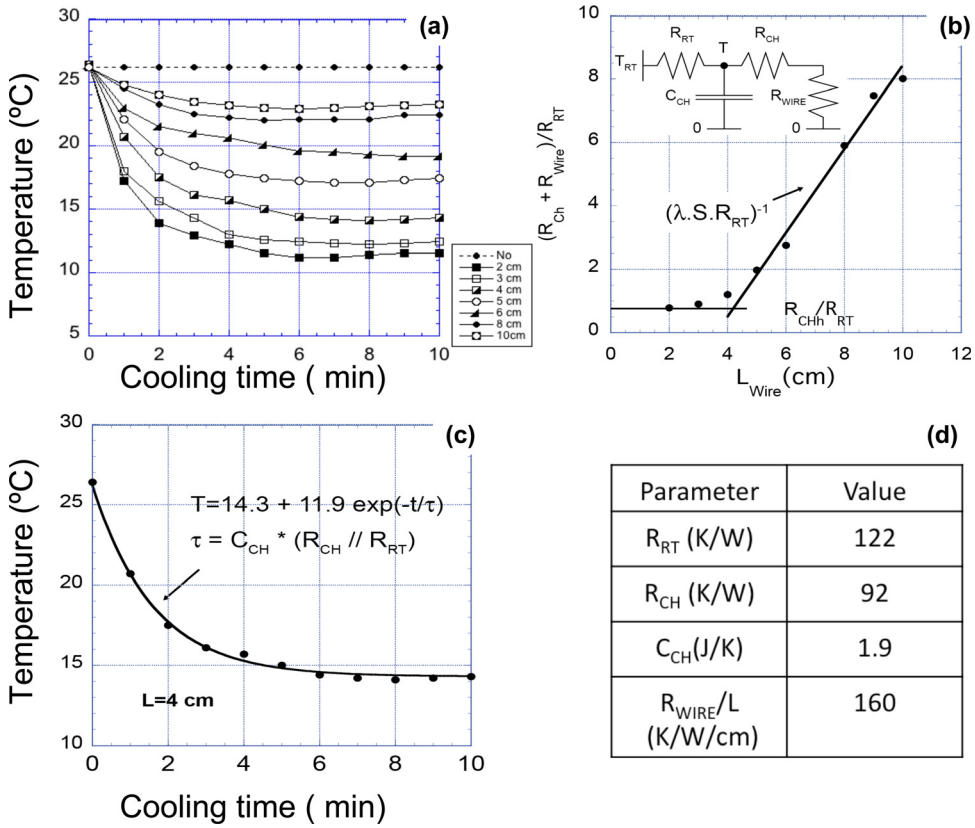

Parameter	Value
R_{RT} (K/W)	122
R_{CH} (K/W)	92
C_{CH}(J/K)	1.9
R_{WIRE}/L (K/W/cm)	160

FIG. 4. Thermal characterization of the chamber. (a) Chamber temperature transients for various wire lengths. (b) Evolution of the thermal resistivity with the wire length from the steady state temperatures given by $(R_{CH}+R_{WIRE})/(R_{RT}+R_{CH}+R_{WIRE})$. (c) Transient temperature cooling with first order extraction for the determination of the response time. (d) Values of the electro-thermal equivalent parameters of the chamber and its cooling system.

Such autocatalytic amplification reaction may start at a lower temperature than it is designed for. In order to efficiently block the reaction at 25 °C (i.e., the temperature of droplet generation), we introduced an "inhibitor" DNA strand.[27] The inhibitor is longer than the target α, hence more stable on the template. Also, the 3′ end of the inhibitor is mismatched, which prevents the polymerase from elongating it (Figure 6(b)). As the temperature is raised to 43 °C, the inhibitor is released, α triggers the reaction and is exponentially amplified (Figure 6(c)).

We first checked that the agarose gel was not hindering the reaction: DNA amplification performed the same in the presence or absence of gelified agarose (see supplemental material, Fig. S3),[28] suggesting that it should be possible to do the reaction in agarose microbeads. A

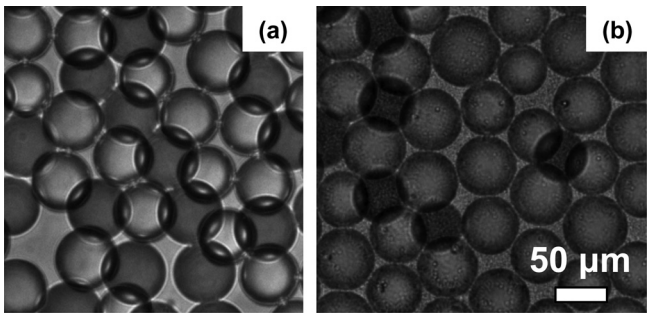

FIG. 5. Agarose microdroplets (a) before and (b) after cooling. After temperature decreases, the microdroplets' opacity increases, suggesting the formation of the agarose mesh (i.e., gelation process).

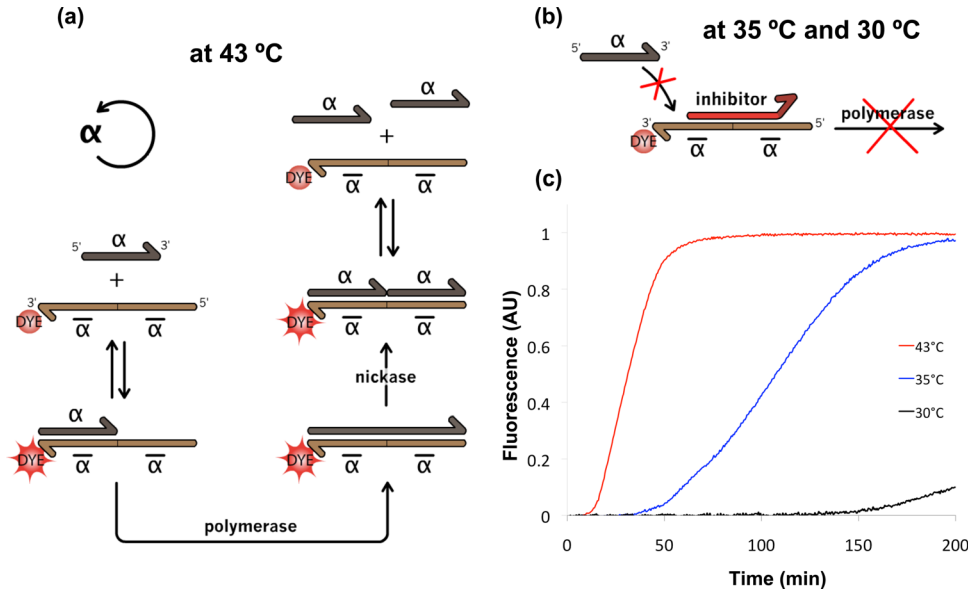

FIG. 6. Autocatalytic DNA amplification reaction in bulk. (a) Schematic of the DNA amplification reaction. At 43 °C, DNA amplification occurs: as strand α hybridizes to the template, it is elongated by DNA polymerase. The nascent strand is cut in its middle by a nicking endonuclease, releasing two α strands. The template's 3′ end is modified with a fluorescent dye, allowing the monitoring of presence of α. (b) At a lower temperature, a stable inhibitor strand blocks the reaction by displacing strand α, and preventing any polymerase activity. (c) Experimental fluorescence time plot of the isothermal DNA amplification in the presence of the inhibitor strand. At a temperature lower than 43 °C, the reaction is slowed down or even blocked by the presence of the inhibitor.

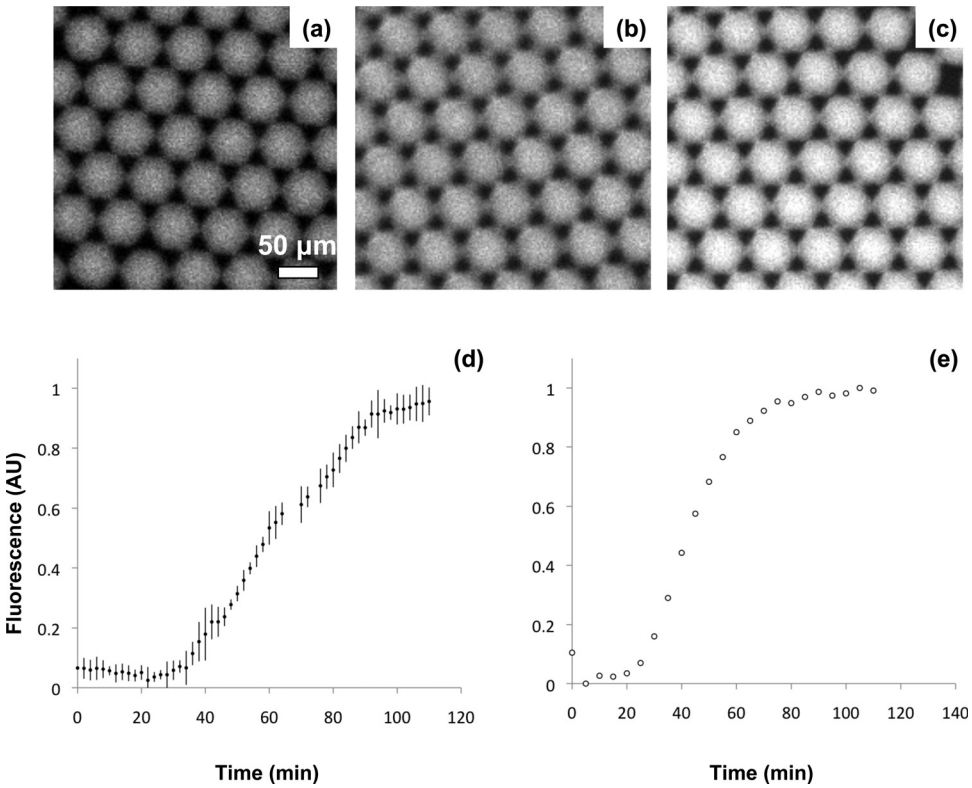

FIG. 7. Autocatalytic DNA amplification in agarose microbeads. Fluorescence in microbeads at (a) 0 min, (b) 60 min, and (c) 110 min. (d) The mean fluorescence ± standard deviation (error bars) of 10 microbeads is plotted to establish a fluorescence variation curve during incubation on-chip. (e) Control experiment (using the same reaction mix) run simultaneously at 43 °C in a thermal cycler.

solution premix containing DNA amplification reagents and 1.5% agarose is prepared at room temperature. Half of the premix is run in a thermocycler as control, and the other part is introduced in the device for microdroplet generation.

The premix deposited in the device inlet is segmented into 55 μm microdroplets. When the incubation chamber is filled with microdroplets, the cooling stage is started, as previously described. Once agarose microbeads are formed, we increased the temperature to 43 °C in order to start the reaction.

This reaction can be monitored by an increase in fluorescence, associated with the amplification of DNA (Figure 7).

In both cases (on-chip and control), the reaction starts after 20 to 30 min of incubation: The fluorescence increases exponentially and saturates after about 60 min. This increase in fluorescence is caused by α strands hybridizing next to the TAMRA fluorophore, and thus represents the amplification of strand α in both microbeads and bulk reaction.

IV. CONCLUSIONS

Agarose microbeads offer a powerful tool for biochemical applications. Previously reported agarose microdroplet generation has been performed by pushing relatively large amount of reagents into the device. Here, for the first time, we have generated agarose microdroplets by using a "push-pull" system. Because the agarose sample is aspirated in the inlet, a few microliters of sample are enough to generate microdroplets. Moreover, the monodisperse agarose microdroplets can be cooled on-chip into agarose microbeads. This design requires no valves and allows (i) biochemical reactions to be performed in microdroplets before or after the gelation process, (ii) on-chip monitoring, and (iii) stabilization of individual droplets into microbeads for facilitated downstream collection and analysis.

As low volumes of sample are required, a potential application of this system could be, by encapsulating single cells, to analyze and sequence the transcriptome.

ACKNOWLEDGMENTS

The authors would like to acknowledge CNRS for financial support and the Institute of Industrial Sciences of the University of Tokyo for laboratory access. The authors would also like to thank Dr. Christophe Provin for helpful discussion and advice and Dr. Kevin Montagne for English corrections.

[1]B. Zheng, L. S. Roach, and R. F. Ismagilov, J. Am. Chem. Soc. **125**(37), 11170–11171 (2003).
[2]T. Hatakeyama, D. L. Chen, and R. F. Ismagilov, J. Am. Chem. Soc. **128**(8), 2518–2519 (2006).
[3]I. Shestopalov, J. D. Tice, and R. F. Ismagilov, Lab Chip **4**(4), 316–321 (2004).
[4]M. Margulies, M. Egholm, W. E. Altman, S. Attiya, J. S. Bader, L. A. Bemben, J. Berka, M. S. Braverman, Y. J. Chen, Z. Chen, S. B. Dewell, L. Du, J. M. Fierro, X. V. Gomes, B. C. Godwin, W. He, S. Helgesen, C. H. Ho, G. P. Irzyk, S. C. Jando, M. L. Alenquer, T. P. Jarvie, K. B. Jirage, J. B. Kim, J. R. Knight, J. R. Lanza, J. H. Leamon, S. M. Lefkowitz, M. Lei, J. Li, K. L. Lohman, H. Lu, V. B. Makhijani, K. E. McDade, M. P. McKenna, E. W. Myers, E. Nickerson, J. R. Nobile, R. Plant, B. P. Puc, M. T. Ronan, G. T. Roth, G. J. Sarkis, J. F. Simons, J. W. Simpson, M. Srinivasan, K. R. Tartaro, A. Tomasz, K. A. Vogt, G. A. Volkmer, S. H. Wang, Y. Wang, M. P. Weiner, P. Yu, R. F. Begley, and J. M. Rothberg, Nature **437**(7057), 376–380 (2005).
[5]M. T. Guo, A. Rotem, J. A. Heyman, and D. A. Weitz, Lab Chip **12**(12), 2146–2155 (2012).
[6]A. B. Theberge, G. Whyte, and W. T. Huck, Anal. Chem. **82**(9), 3449–3453 (2010).
[7]M. Zagnoni and J. M. Cooper, Methods Cell Biol. **102**, 25–48 (2011).
[8]B. T. Kelly, J. C. Baret, V. Taly, and A. D. Griffiths, Chem. Commun. (Cambridge) **2007**(18), 1773–1788.
[9]R. Tewhey, J. B. Warner, M. Nakano, B. Libby, M. Medkova, P. H. David, S. K. Kotsopoulos, M. L. Samuels, J. B. Hutchison, J. W. Larson, E. J. Topol, M. P. Weiner, O. Harismendy, J. Olson, D. R. Link, and K. A. Frazer, Nat. Biotechnol. **27**(11), 1025–1031 (2009).
[10]B. E. Debs, R. Utharala, I. V. Balyasnikova, A. D. Griffiths, and C. A. Merten, Proc. Natl. Acad. Sci. U. S. A. **109**(29), 11570–11575 (2012).
[11]T. Rossow, J. A. Heyman, A. J. Ehrlicher, A. Langhoff, D. A. Weitz, R. Haag, and S. Seiffert, J. Am. Chem. Soc. **134**(10), 4983–4989 (2012).
[12]Y. Zeng, R. Novak, J. Shuga, M. T. Smith, and R. A. Mathies, Anal. Chem. **82**(8), 3183–3190 (2010).
[13]H. Zhang, G. Jenkins, Y. Zou, Z. Zhu, and C. J. Yang, Anal. Chem. **84**(8), 3599–3606 (2012).
[14]A. Fallah-Araghi, J. C. Baret, M. Ryckelynck, and A. D. Griffiths, Lab Chip **12**(5), 882–891 (2012).
[15]X. Leng, W. Zhang, C. Wang, L. Cui, and C. J. Yang, Lab Chip **10**(21), 2841–2843 (2010).
[16]W. Y. Zhang, W. Zhang, Z. Liu, C. Li, Z. Zhu, and C. J. Yang, Anal. Chem. **84**(1), 350–355 (2012).

[17]A. Kumachev, J. Greener, E. Tumarkin, E. Eiser, P. W. Zandstra, and E. Kumacheva, Biomaterials **32**(6), 1477–1483 (2011).
[18]Y. J. Eun, A. S. Utada, M. F. Copeland, S. Takeuchi, and D. B. Weibel, ACS Chem. Biol. **6**(3), 260–266 (2011).
[19]J. C. Baret, F. Kleinschmidt, A. El Harrak, and A. D. Griffiths, Langmuir **25**(11), 6088–6093 (2009).
[20]Y. N. Xia and G. M. Whitesides, Angew. Chem., Int. Ed. **37**(5), 551–575 (1998).
[21]J. C. McDonald, D. C. Duffy, J. R. Anderson, D. T. Chiu, H. Wu, O. J. Schueller, and G. M. Whitesides, Electrophoresis **21**(1), 27–40 (2000).
[22]A. Edelstein, N. Amodaj, K. Hoover, R. Vale, and N. Stuurman, Curr. Protoc. Mol. Biol. **14**, 20 (2010).
[23]Z. H. Nie, M. S. Seo, S. Q. Xu, P. C. Lewis, M. Mok, E. Kumacheva, G. M. Whitesides, P. Garstecki, and H. A. Stone, Microfluid. Nanofluid. **5**(5), 585–594 (2008).
[24]J. Y. Xiong, J. Narayanan, X. Y. Liu, T. K. Chong, S. B. Chen, and T. S. Chung, J. Phys. Chem. B **109**(12), 5638–5643 (2005).
[25]G. T. Walker, M. C. Little, J. G. Nadeau, and D. D. Shank, Proc. Natl. Acad. Sci. U. S. A. **89**(1), 392–396 (1992).
[26]A. Padirac, T. Fujii, and Y. Rondelez, Nucleic Acids Res. **40**(15), e118 (2012).
[27]K. Montagne, R. Plasson, Y. Sakai, T. Fujii, and Y. Rondelez, Mol. Syst. Biol. **7**, 466 (2011).
[28]See supplemental material at http://dx.doi.org/10.1063/1.4758460 for the control experiments in agarose and for COMSOL simulation of the temperature in the chamber of the device.